**CSIRO** PUBLISHING
www.publish.csiro.au/journals/ajar *Australian Journal of Agricultural Research*, 2007, **58**, 316–325

# Estimating crop area using seasonal time series of Enhanced Vegetation Index from MODIS satellite imagery

*A. B. Potgieter*[A,E], *A. Apan*[B], *P. Dunn*[C], *and G. Hammer*[D]

[A]Emerging Technologies, Queensland Department of Primary Industries & Fisheries, Toowoomba, Qld 4350, Australia.
[B]Australian Centre for Sustainable Catchments & Faculty of Engineering and Surveying University of Southern Queensland, Toowoomba, Qld 4350, Australia.
[C]Australian Centre for Sustainable Catchments & Faculty of Sciences, University of Southern Queensland, Toowoomba, Qld 4350, Australia.
[D]School of Land and Food Sciences, The University of Queensland, Brisbane, Qld 4072, Australia.
[E]Corresponding author. Email: andries.potgieter@dpi.qld.gov.au

**Abstract.** Cereal grain is one of the main export commodities of Australian agriculture. Over the past decade, crop yield forecasts for wheat and sorghum have shown appreciable utility for industry planning at shire, state, and national scales. There is now an increasing drive from industry for more accurate and cost-effective crop production forecasts. In order to generate production estimates, accurate crop area estimates are needed by the end of the cropping season. Multivariate methods for analysing remotely sensed Enhanced Vegetation Index (EVI) from 16-day Moderate Resolution Imaging Spectroradiometer (MODIS) satellite imagery within the cropping period (i.e. April–November) were investigated to estimate crop area for wheat, barley, chickpea, and total winter cropped area for a case study region in NE Australia. Each pixel classification method was trained on ground truth data collected from the study region. Three approaches to pixel classification were examined: (*i*) cluster analysis of trajectories of EVI values from consecutive multi-date imagery during the crop growth period; (*ii*) harmonic analysis of the time series (HANTS) of the EVI values; and (*iii*) principal component analysis (PCA) of the time series of EVI values. Images classified using these three approaches were compared with each other, and with a classification based on the single MODIS image taken at peak EVI. Imagery for the 2003 and 2004 seasons was used to assess the ability of the methods to determine wheat, barley, chickpea, and total cropped area estimates. The accuracy at pixel scale was determined by the percent correct classification metric by contrasting all pixel scale samples with independent pixel observations. At a shire level, aggregated total crop area estimates were compared with surveyed estimates. All multi-temporal methods showed significant overall capability to estimate total winter crop area. There was high accuracy at pixel scale (>98% correct classification) for identifying overall winter cropping. However, discrimination among crops was less accurate. Although the use of single-date EVI data produced high accuracy for estimates of wheat area at shire scale, the result contradicted the poor pixel-scale accuracy associated with this approach, due to fortuitous compensating errors. Further studies are needed to extrapolate the multi-temporal approaches to other geographical areas and to improve the lead time for deriving cropped-area estimates before harvest.

**Additional keywords:** multi-temporal MODIS, harmonic analysis, principal component analysis.

## Introduction

Cereal grain is one of the main agricultural export commodities of Australia. Grain production, particularly wheat, has increased rapidly during the latter part of the 20th Century (Knopke *et al*. 2000). This has increased the need of government bodies and industry for crop production forecasts at various spatial and temporal scales. In Australia, variability in cereal production is chiefly affected by climate variability (Nix 1975). This variability can generate significant macro-economic consequences. For example, the severe drought of 2002 reduced the economic growth of the Australian economy by ~0.75 percentage points (Penm 2002). During the last decade, numerous objective information tools have been developed to assist agri-industry in managing this variability at the paddock/farm level (Hammer *et al*. 2001; Nelson *et al*. 2002) and at the regional level (Stephens *et al*. 2000; Potgieter *et al*. 2002, 2005). Having access to such decision-support tools has become increasingly necessary to better deal with production risk in such a highly variable environment.

An example of such an objective information tool is the Regional Commodity Forecasting System (RCFS), which is being used operationally by the Queensland Department of Primary Industries & Fisheries (QDPI&F) to predict shire-scale wheat and sorghum yield on a monthly basis (www.dpi.qld.gov.au/fieldcrops). This system, which has operated since 1999, generates a forecast yield distribution for

 10.1071/AR06279 0004-9409/07/040316

wheat and sorghum on a monthly basis through the cropping season. The system involves the integration of an agro-climatic-based simple crop stress index model (Stephens 1998; Potgieter *et al*. 2005, 2006), weather data for the season up to the time of the forecast, and an El Niño Southern Oscillation (ENSO)-based seasonal climate forecast system (Stone *et al*. 1996) for the remainder of the season. The RCFS is run each month throughout the crop-growing seasons (winter and summer) for all main crop-production shires in Australia. A shortcoming of this system, however, is that it generates only a yield per unit area estimate. To estimate total production, decision makers must combine this with their subjective knowledge of total area sown (to be harvested) at a spatial scale. Thus, in order to generate total-production predictions, a real-time or near real-time estimate of the cropping area is needed throughout the cropping season. Production predictions can be used in updating supply-chain information at the regional, state and national levels.

Currently, no real-time objective estimates of end-of-season shire-scale cropped area estimates exist. Although the Australian Bureau of Statistics (ABS) collates an annual shire-scale survey, these data are usually not available until up to 2 years after the survey/census. The use of satellite information, therefore, offers more objectivity, timeliness, repeatability and accuracy. Up to now, however, remote-sensing-based regional crop-production forecasting systems have not become operational at a regional scale mainly because of the high resource costs (i.e. imagery, computer disk space, and speed) and the tediousness of applying fine-resolution imagery to large areas. With the advent of MODIS imagery, from the satellites launched in December 1999 and May 2000 (i.e. the Terra platform, which captures morning images, and the Aqua platform, which captures afternoon images, respectively), there is a potential to address the issues of cost and useable pixel size for regional applications.

In this study, we examine the use of MODIS imagery to derive specific crop-area estimates for agricultural forecasting systems aimed at estimating crop production at a regional scale. Various studies have used MODIS in determining land-use patterns (Muchoney *et al*. 2000; Zhan *et al*. 2002; Price 2003), vegetation phenology (Zhang *et al*. 2003), and crop (rice) production in the Northern Hemisphere (Xiao *et al*. 2005). Near real-time MODIS imagery has also been used in the crop explorer framework developed by the United States Department of Agriculture (USDA), which uses accumulated Normalised Difference Vegetation Index (NDVI) to describe crop conditions relative to a base year (see www.pecad.fas.usda.gov/cropexplorer). This system generates vegetation-canopy condition indices at an aggregated continental scale for high-level decision makers. Such a non-crop specific (i.e. generalised vegetation-canopy condition) approach is likely to have limited value to industry where commodity management decisions need to be made at a much finer spatial resolution (e.g. shire scale). Currently, no near real-time crop-specific area estimates exist for crop-specific agricultural systems at a shire scale in Australia.

The main objective of this study was to determine the utility of multi-temporal MODIS satellite imagery in estimating area of specific and total winter crops at the end of any specific cropping season. This was achieved by contrasting 3 multivariate approaches to analyse time series of enhanced vegetation index (EVI) temporal profiles throughout the cropping period. Pixel and shire-scale accuracies for each season studied were assessed based on in-season ground truthing, using data for 2 selected shires in the Darling Downs region, Queensland, Australia. For each analysis method, pixel classification was trained on ground truth data and accuracy tested on an independent set of ground truth data and on survey data at the aggregate shire scale.

## Methods

### *Study area*

The study area is located in the central Darling Downs region, ~150 km west of Brisbane, Queensland, Australia (Fig. 1). The Jondaryan and Pittsworth shires (~200 000 ha) were selected for this study. The typical crop area planted in both shires equates to nearly half of the total potential cropping area during either winter or summer cropping seasons. Crop management practices are variable, and paddock sizes can range from small (~20 ha) to very large (>400 ha). Some larger paddocks might be divided into cropping strips. These strips can vary in width from 50 to 180 m in some areas and are usually used in crop rotation practices. The practice of strip cropping was introduced as a preventative measure to counteract the potential loss of topsoil via water runoff and erosion during wet seasons. Soils in this region are generally deep and high in clay content and therefore have very high potential soil water-holding capacities. In addition, the high variability in in-crop (i.e. May–October period) rainfall[1], combined with the advantage of deep soils and high soil moisture-storing capacity, has shaped crop-management practices in the northern region to be more dependent on starting soil moisture at sowing than regions further south in the more winter-dominant rainfall areas (Nix 1975). The summer-dominant rainfall makes the region highly suited to summer cropping and the soil storage capacity also makes it favourable for winter cropping (e.g. wheat, barley and chickpea), with sowing occurring between middle of April and the end of June. Rotations traditionally incorporate both winter and summer crops. In these shires, land-use patterns over the last 10 years have been dominated by cropping (78% of total shire area in both shires), with total winter crop area planted (which includes wheat and barley) very similar to summer crop area planted (which includes sorghum and cotton) (www.nrm.qld.gov.au/).

Spatial crop yield variability within a specific season can be caused by either variability in rainfall amount, soil type, crop management practices, timing of rainfall, or any combination of these factors. Although variability in rainfall amount might be small across the study area in some years (e.g. 2004), there is significant variability in the other factors, constituting a heterogeneous spatial cropping landscape. This was evident in the differences in aggregated shire wheat and barley yields of 2.96 and 2.69 t/ha for the 2003 season for the Jondaryan and Pittsworth shires, respectively. Differences in aggregated shire

[1] Coefficient of variation for in-crop (i.e. May–October period) shire rainfall was >46% for the period 1977–2004, with rainfall station data weighted within a shire based on area represented.

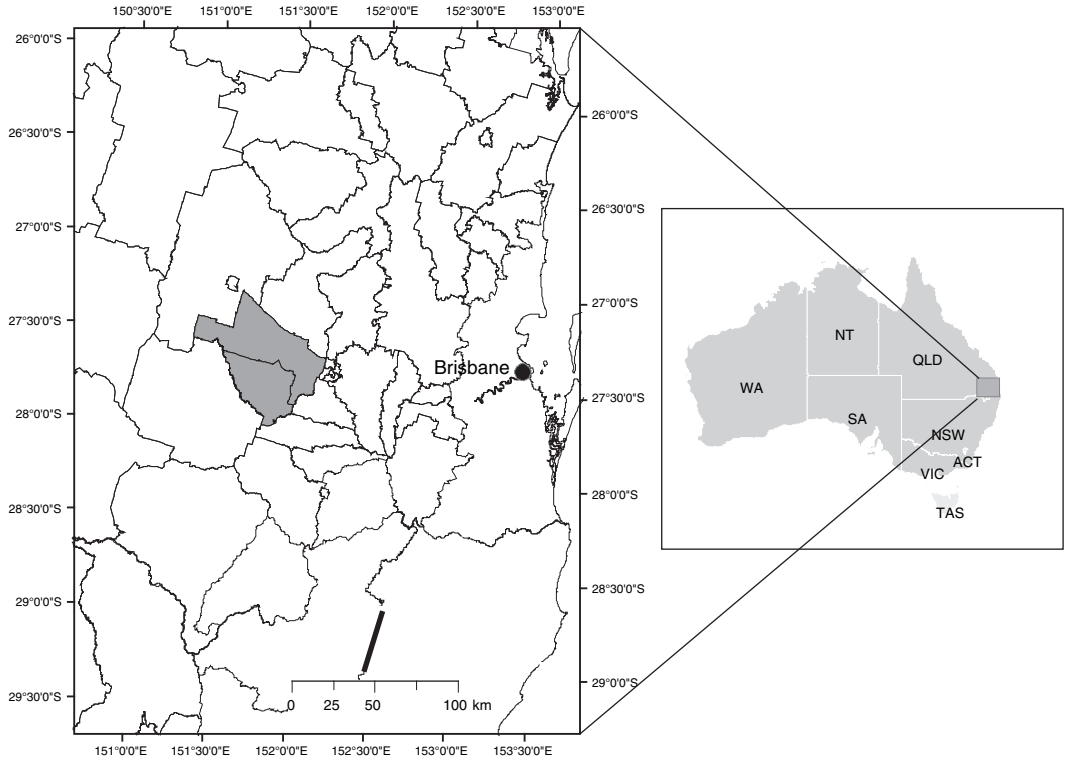


**Fig. 1.** Location of the Jondaryan and Pittsworth shires (hatched in black) within the north-eastern region of Australia. Shire boundaries are given by black solid lines.

wheat and barley yields were less during drier seasons such as 2004, with 2.52 and 2.5 t/ha for the Jondaryan and Pittsworth shires, respectively (ABARE 2005).

### *Vegetation index*

The 16-day MODIS EVI imagery, which is derived from transformations of the red (620–670 nm, 250 m pixel size), near-infrared (NIR, 841–876 nm, 250 m pixel size), and blue (459–479 nm, 500 m pixel size) spectral bands, was used to form a continuous time series of data that represented the crop growth EVI temporal curve for each pixel in the study area. The MODIS EVI was selected for its insensitivity to atmospheric and canopy soil background noise. In addition, it optimises the vegetation signal with improved sensitivity at higher biomass, which is a significant improvement on the traditional NDVI measure (Huete *et al*. 2002).

The EVI is computed as:

$$\mathrm{EVI} = G\frac{\rho_{\mathrm{NIR}} - \rho_{\mathrm{R}}}{\rho_{\mathrm{NIR}} + C_1\rho_{\mathrm{R}} - C_2\rho_{\mathrm{B}} + L} \qquad (1)$$

where ρ is the atmospherically corrected or partially atmospherically corrected (Rayleigh and ozone absorption) surface reflectances; $L$ is the canopy background adjustment that addresses non-linear, differential NIR and red radiant transfer through a canopy; and $C_1$ and $C_2$ are the coefficients of the aerosol resistance term, which uses the blue band to correct for aerosol influences in the red band (Huete *et al*. 2002). The coefficients adopted are $L = 1$, $C_1 = 6$, $C_2 = 7.5$, and $G = 2.5$, which represents a gain factor (Huete *et al*. 1994, 1997). The EVI values thus have an extended sensitivity, which makes it more likely to discriminate among canopy structure differences, such as leaf area index (LAI) differences (Justice *et al*. 2002). The EVI is MODIS specific and is composed based on high-quality EVI values during the 16-day cycle. A filter to the data is applied, which is based on quality, cloud cover and viewing angle in order to create the high-quality EVI values (Huete *et al*. 2002). The MODIS EVI values range from −2000 to 10 000, with a scale factor of 10 000, and have a fill value for missing data of −3000. On this scale, water bodies have a negative EVI value or close to zero, while canopy cover has positive EVI values up to a maximum of 10 000 (dense forest canopy).

### *Satellite imagery and re-projection*

The 'MOD13Q1' MODIS satellite product, which includes the 16-day 250-m VI data, was downloaded from NASA's Earth Observing System (EOS) (http://edcimswww.cr.usgs.gov/pub/imswelcome/) website for the period 2003–04. This resulted in 46 images (i.e. 23 images × 2 years) each of which had a file size of 500 megabytes. The 23 images within each season were downloaded for the period January–December. The NDVI and EVI MODIS products were geometrically, atmospherically, and bidirectional reflectance distribution fraction (BRDF) corrected, validated, and quality assured through the EOS program (Huete *et al*. 2002; Justice *et al*. 2002). The MODIS reprojecting tool (http://edcdaac.usgs.gov/datatools.asp) was used to subsample the 'granule' to an area covering the study area. An image was created by stacking the 23 images for each

season with a GDA94 projection in ENVI software (RSI 2005), thus creating a single image with 23 layers. This resulted in a continuous sequence of EVI temporal values for each pixel for each season.

Landsat TM 5 images (14 and 16 Sept. 2004), in combination with farm boundaries and the 1999 land-use map (Department of Natural Resources and Water 2006) of the study area, were used to assure that selected ground truth points were 'pure', i.e. each selected pixel was near the centre of a paddock and that the pixels were mainly from large paddocks.

### *Multi-temporal analysis methods for EVI time series*

Major constraints in the use of medium to high resolution satellite imagery for estimating crop area or yield are aligning the image date with maximum crop canopy cover during the crop growth period, and the high costs involved in acquiring such imagery. This is further confounded by variability in climate, soil and crop practices within a specific region, making crop yield and area estimates less accurate and more tedious to compute. To overcome this problem in this study, we focussed on the use of multiple consecutive images spanning the whole calendar year (i.e. January–December). This allowed the capture of crop canopy information before, during, and after the crop growth period.

The efficacy of 3 analytical approaches to the multi-temporal data was examined: (*i*) clustering of multi-date MODIS EVI (MEVI) image values between day of year (DOY) 97 (early April) and DOY 305 (end of October); (*ii*) harmonic analysis of the time-series (HANTS) (Jakubauskas *et al*. 2001, 2002) of EVI data; and (*iii*) Principal Component Analysis (PCA) of the time series of EVI data. The methods were assessed based on their ability to correctly classify image pixels based on field observations over a period of 2 years (2003 and 2004) and the degree of association with surveyed shire-scale crop area data (ABARE 2005).

The first approach involves classifying EVI values from the consecutive MODIS imagery during the main winter crop-growth period, which spans from early April to late October in this region. This constitutes the MEVI approach.

The second approach (HANTS) is based on decomposing the time series of EVI data from the imagery into harmonic components or terms. In this study, for each pixel within the study area, the time series encompassing 23 16-day MODIS EVI composites in each year was decomposed using a discrete Fast Fourier Transform algorithm into a set of amplitude and phase terms at different temporal frequencies. This technique was applied through the use of the Harmonic Analysis of Time Series software (Verhoef *et al*. 1996).

Thirdly, the PCA approach uses traditional multivariate analysis to reduce the multidimensional complexity in the temporal EVI profile. In this study, PCA (Richards and Jia 1999; Campbell 2002; Davis 2002) was used to reduce the EVI time series at each pixel from the 23-image sequence into a smaller set of transformed variables or principal components (PC), which explained 90% or more of the temporal variability in the series.

Finally, a benchmark (or control) classification approach was included. This was derived from a single-date EVI MODIS image acquired around the peak of the average EVI (PEVI) profile. In the analysis, peak EVI was selected at DOY 225.

### *Crop/image feature classes and pixel classification*

For each analysis method, pixel classification was trained on ground truth data and its accuracy tested on an independent set of ground truth data. Ground truth data were collated during field trips undertaken in each year. In total, 1302 (wheat = 252; barley = 96; chickpea = 36; other = 918) and 1365 (wheat = 243; barley = 45; chickpea = 9; other = 1068) sampling points were selected from the ground truth data for the 2003 and 2004 season, respectively. Locations sampled within the study area were classified according to crop/feature classes (i.e. wheat planted early, wheat planted late, barley, etc.) given in Table 1. All features were identified from ground truth data gathered during field trips except for the vegetation and forest classes, which were identified from the 1999 land-use map (Department of Natural Resources and Water 2006). The feature class selections encompass classes of main interest, i.e. wheat, barley, and chickpea.

The ability to discriminate among crops is directly related to the amount of reflectance, specifically in the NIR bandwidth, by the leaf and canopy structures (Campbell 2002). For wheat and barley, these features are very similar. The main factor contributing to differences in canopy reflectance between wheat and barley relates to canopy architecture and density, which is a function of the number of tillers and rate of growth. For barley, tillering and early growth are nearly double those of wheat, causing more rapid crop canopy closure (Meinke *et al*. 1998). This is a significant feature because discriminatory ability is likely to be associated with this attribute. The different crop architecture and phenology of chickpea cause its leaf and canopy structure development to be almost in all cases quite different from wheat and barley, thus enabling discrimination between these crops.

The inclusion of crop feature classes or merging of specific classes was determined using separability metrics such as the Jeffries-Matusita (JM) measure. This metric constitutes the separability between 2 feature classes and is a function of

**Table 1. Feature classes and data collating method used in the first level of classification for 2003 and 2004 seasons**

*Double cropped* represents cropping in consecutive summer and winter seasons; *fed off* is traditionally hayed or grazed; *late plantings* are usually plantings occurring at the end or after the close of the traditional wheat planting window; n.a. represents no available data

| Feature class | 2003 | 2004 |
|---|---|---|
| Barley | Field trip | Field trip |
| Barley double cropped | Field trip | n.a. |
| Barley fed off | Field trip | n.a. |
| Chickpeas | Field trip | Field trip |
| Grazing & natural vegetation | Field trip & land use map | Field trip & land use map |
| Natural forest | Land use map | Land use map |
| Production forest | Land use map | Land use map |
| Stubble & soil | Field trip | Field trip |
| Wheat | Field trip | Field trip |
| Wheat late plantings | Field trip | n.a. |

the average distance between the spectral means of 2 classes. Output values range from 0 to 2.0 and indicate how well the selected feature class pairs are statistically separate. Values greater than 1.9 indicate that the feature class pairs have good separability (Richards and Jia 1999).

Supervised classification was performed via the maximum likelihood classification (MLC) algorithm (Richards and Jia 1999), which was available as part of the ENVI software. When only one layer or band was used, as in the case of the PEVI approach, the minimum distance classifier (MDC) method was used. The classifiers (i.e. MLC and MDC) were trained using 'pure' pixels within the ground truth data sample set (i.e. those pixels that fall completely within a large and homogeneous paddock for a specific feature type).

### *Independent validation and accuracy assessment*

The accuracy of classification was assessed by contrasting the classified image (as described in the previous section) with independent randomly selected subsamples from the ground truthing (collated through field trips). This was done to reduce artificial accuracy, i.e. minimise classification bias. In total, 316 and 344 independent random ground truth pixels were selected and used to calculate accuracy for the 2003 and 2004 seasons, respectively. This represented ~25% of the total ground truth samples in each year. The proportion of pixels correctly classified was expressed empirically in a contingency table known as the confusion or error matrix. The statistic, percent correctly classified (PCC), was used to determine the overall and between-crop accuracies for each classification approach (Richards and Jia 1999). The results allowed inferences about the comparative discriminatory ability of the multi-temporal decomposition approaches used in this study.

Accuracy at the aggregate shire scale was determined by comparing derived estimates of total and specific winter crop area with results of extended farm surveys conducted in the study region for the 2003 and 2004 seasons (ABARE 2005). The degree of correspondence within a specific season at a shire scale was measured by calculating the percent error (PE). PE is computed as the ratio of the difference of the remotely sensed area estimate and the surveyed area estimate to that of the surveyed area estimate for each method for each year within a shire. The mean of the absolute PE was calculated to determine the accuracy across seasons and shires (MAPE).

## Results and discussion

### *Feature class selection*

The temporal separability between class means of wheat and wheat late plantings was moderate (JM = 1.6) when the distance measures were compared. Hence, all wheat samples were merged into one feature class with 252 and 243 sampling points in 2003 and 2004, respectively. Although good separability was evident between barley/barley double cropped (JM = 1.99) and barley/barley fed off (JM = 1.99), both barley double cropped and barley fed off were excluded from the final classification. This was mainly because double cropping and fed off and haying of crops are less common practice and resulted in fewer training and independent sampling points for ground truthing. This resulted in 96 and 45 sampling points in 2003 and 2004, respectively. Very few chickpea sites were observed and selected in either season, mainly because very little area was sown to chickpea, especially in the 2004 season. Although there were few sampling points for chickpea (36 in 2003 and 9 in 2004) it was retained as a separate class to assess the discriminatory ability of the proposed methods between the 2 main winter crops (i.e. wheat and barley), and the less important winter crop (i.e. chickpea). The separability between barley and chickpea was larger than that between wheat and chickpea. For simplicity, all other features (e.g. vegetation, natural forest, bare fallow, etc.) were combined to form one feature class with 918 and 1068 sampling points for both seasons. In total, 4 main feature classes (i.e. wheat, barley, chickpea and non-cropping) were formed for further analysis and classification.

### *Temporal crop EVI profiles*

The average temporal EVI profiles throughout each growing season showed distinct differences for wheat, barley and chickpea (Fig. 2). The profiles represent the temporal plant-canopy responses to soil, plant and water regime combinations within the study area for each season. The differences among crops in slope of the temporal profiles from emergence (i.e. EVI >2000 after DOY 129) to anthesis (i.e. flowering around peak EVI at DOY 225) were more evident during 2003 than in 2004.

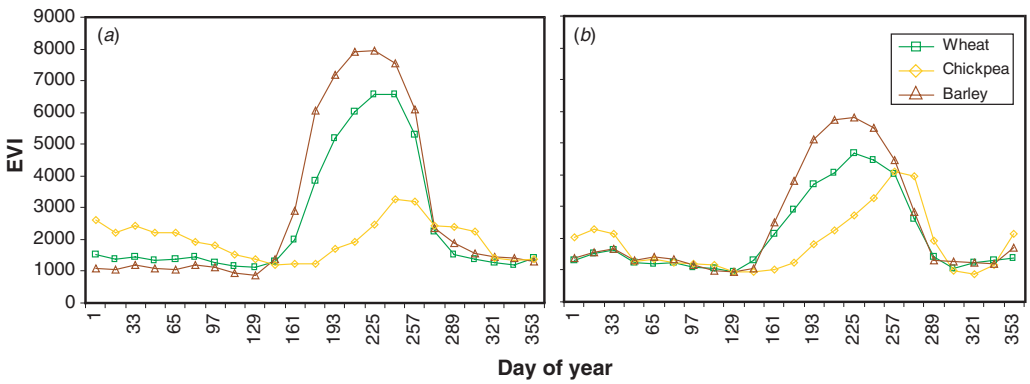


**Fig. 2.** Average temporal EVI profile throughout the growing season for wheat (square), barley (triangle) and chickpea (diamond) for (*a*) 2003 winter crop season and (*b*) 2004 winter crop season.

The period from crop emergence to anthesis is known as the green-up period and the period after anthesis to crop harvest is known as the senescence period. The temporal profiles for barley and wheat suggested a very similar planting date as crop emergence was around the same time for both seasons for both shires (Fig. 2). The average crop emergence date of chickpea was at least 2 months after that of wheat and barley, which suggested a later average planting date in both seasons within the study area.

The average EVI temporal profile for barley was higher than that of wheat in both seasons. In addition, the green-up rate for barley was quicker than that of wheat in both seasons, which was mainly an effect of the higher (i.e. nearly double) tillering and early leaf area growth rate of barley (Meinke *et al*. 1998). There were, however, some instances where the green-up rate of wheat was similar to that of barley. This could be possibly ascribed to differences in soil temperatures, increased nitrogen levels, or no water limitations (e.g. irrigated) (Meinke *et al*. 1997). Conversely, chickpea had much lower average EVI values than that of wheat and barley in both seasons. The differences in average peak EVI values were not as large for the 2004 season. Although there was some overlap in the temporal profile distributions between crops, the differences in the shape of the profiles among wheat, barley and chickpea were apparent for both seasons. The much lower EVI peaks for wheat and barley during the 2004 season were mainly caused by the significantly below-average rainfall recorded during 2004, which resulted in a reduction in biomass and crop growth and thus ensuing lower EVI values. During periods of severe moisture stress such as in 2004, the reflectance of crops in the visible (blue, green and red) bands increases (due to less absorption by chlorophyll), whereas reflectance in the near-infrared band decreases, resulting in smaller band ratio values and ensuing EVI values. Some overlaps in EVI temporal profile distributions for wheat, barley and chickpea indicate that there will be some confusion in separating these crops, and consequently some pixels will likely be wrongly classified.

### *Image classification*

Once each method was trained on ground truth data, classification of all pixels on the image was done by applying the standard maximum likelihood classifier for the multi date EVI imagery (from DOY 97 to 305) and the derived PCA and HANTS imagery. The minimum distance classifier was used to classify the peak EVI approach at DOY 225 (PEVI). For the PCA approach, 11 principal components were retained, which explained more than 90% of the total temporal variability in the time series derived from the 23 images. For the HANTS approach, 3 harmonic terms (each term consists of a phase and amplitude value) and the zero amplitude were used in the final classification. This included the EVI average (0th harmonic), first, second and third harmonics (amplitude and phase for each harmonic). The three harmonics plus the average explained more than 90% of the temporal variability, similar to the finding for the PCA approach.

Figure 3 shows the classified images using the PEVI (*a*, *b*) and HANTS (*c*, *d*) approaches for the 2003 and the 2004 seasons, respectively. In general, the 2 seasons differ significantly in the amount of total winter crops planted. Independent of the classification approach, more winter crop was evident in 2003 than in 2004. This related mainly to the poor rainfall recorded during 2004 and the lack of sowing opportunities during the winter crop planting window (i.e. May–June). In addition, the PEVI approach overestimated chickpea occurrence in both seasons, with many of the non-cropping pixels classified as chickpea in both 2003 and 2004 (*a*, *b*). The HANTS approach showed substantially better discriminatory ability among wheat, barley, chickpea, and non-cropping than the PEVI approach in both seasons. This was due to the better discriminatory ability of the HANTS approach compared with that of the single-date approach at pixel scale (Table 2). Similar results to those for the HANTS approach were found for the MEVI and PCA data reduction methods (data not shown).

### *Independent validation and accuracy assessment*

The percentage of pixels correctly classified (PCC) for each of the 4 methods is given in Table 2. The overall accuracy among these methods ranged from 56 to 98%. The single-date approach (PEVI) had most pixels incorrectly classified with an overall accuracy of 56 and 61% for 2003 and 2004 seasons, respectively. Most of this error came from misclassifying wheat and non-cropping classes during both seasons. The overall PCC values for the multi-temporal approaches were all very high, with the highest accuracies produced in 2004. All multi-temporal approaches classified the non-cropping pixels correctly (100%). This is significant because it means that such approaches can be effectively used to discriminate crops from non-cropping land-use areas in future studies. All multi-temporal approaches achieved much higher overall accuracy compared with the single-date method for both the 2003 and 2004 seasons. This is mainly a result of the better ability in discriminating between wheat, barley, chickpea and non-cropping in both seasons by utilising the temporal canopy signatures derived from the entire crop growth period.

Comparing the total winter crop area estimates (i.e. wheat, barley and chickpea) with the surveyed shire-scale data as collated by ABARE (Table 3), the HANTS method produced the smallest error (i.e. highest accuracy) within the Jondaryan shire for both seasons. It has an average mean absolute percent error (MAPE) of 26% (PE of 18% and −35% for each season, respectively). The MAPE across both shires was 27% (Table 4). All other methods showed MAPE greater than 63% for the Jondaryan shire (Table 3) and 97% across both shires for both seasons (Table 4). The single-date method had the lowest PE for total wheat area estimated of 5 and 9% for the Jondaryan shire for 2003 and 2004, respectively. This result, however, is fortuitous because of the very poor overall and within-class pixel accuracies (Table 1). This artificial accuracy of the single-date approach is further confirmed by the very poor total winter crop shire-scale accuracy within 2003 (182%), 2004 (268%), and overall (225%) (Table 4). The high accuracy for the single-date wheat classification at an aggregated shire-scale is therefore spurious because of compensating errors when aggregating. Furthermore, the single-date approach is compounded by the question of

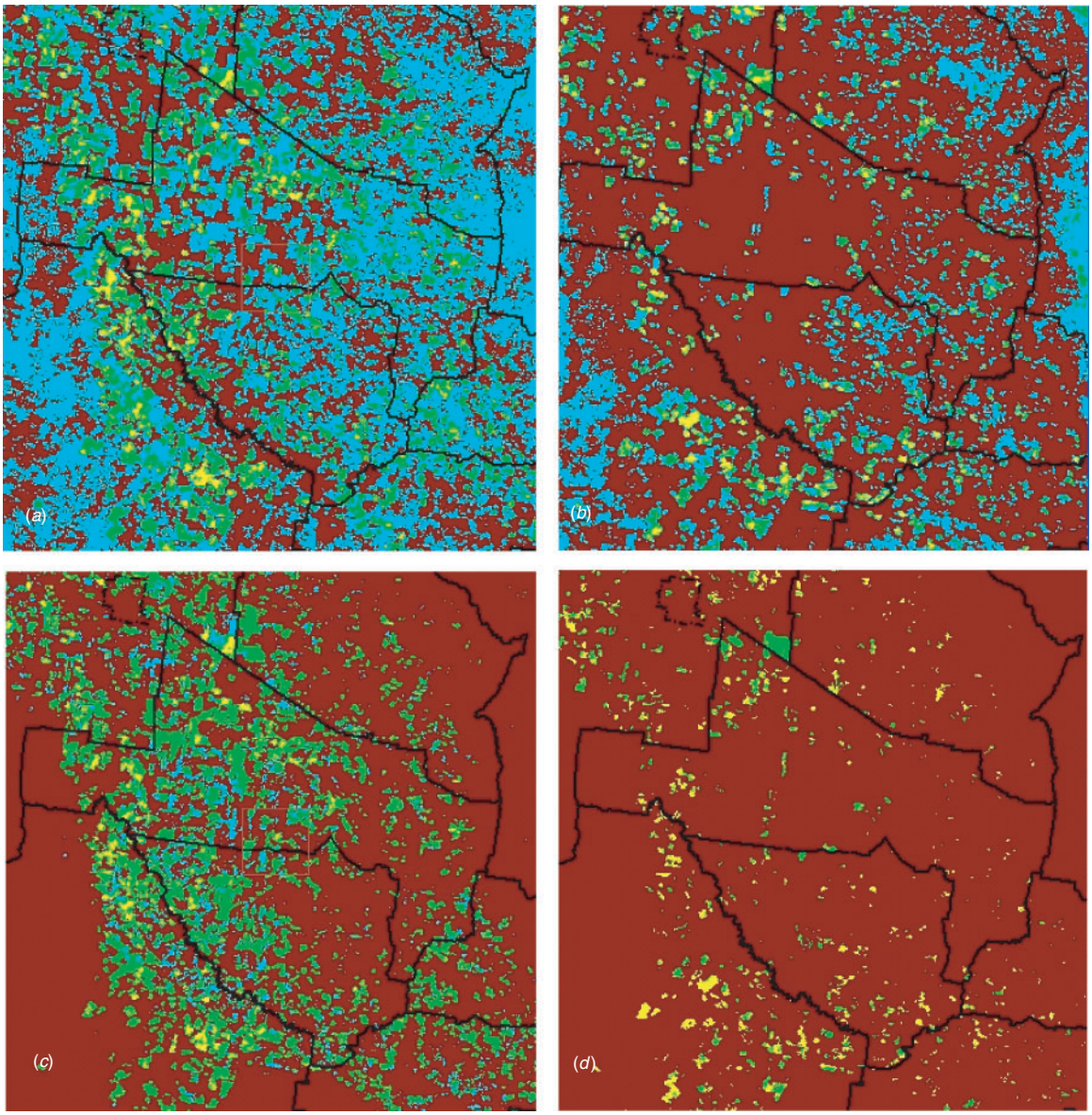


**Fig. 3.** Classified images using the PEVI classification for the 2003 and 2004 seasons (*a*, *b*) and classified images using the HANTS approach for 2003 and 2004 seasons respectively (*c*, *d*). Wheat is coloured in green, barley in yellow, chickpea in cyan and non crop (e.g. natural and production forest, vegetation, stubble, bare soil, etc.) in brown.

the best date to use, which cannot be readily determined until after the season. Therefore the single-date approach cannot be recommended as an acceptable method for determining winter crop area at a regional scale.

The HANTS approach showed moderate to high within-season accuracy for total winter crop area estimates, with MAPE values of 33 and 21% for the 2003 and 2004 seasons, respectively (Table 4). All multi-temporal approaches showed significantly higher accuracy at the aggregated shire-scale level within and across seasons compared with the accuracy of the single-date approach. The HANTS method had the highest overall accuracy (27%) when determining total winter crop area estimates across seasons within the study area.

Although the HANTS approach showed overall pixel accuracy similar to that of the other multi-temporal approaches, it had the smallest total winter crop area error across both seasons and is thus likely to be more reliable than any of the other analysis approaches. The shire-scale accuracy of HANTS could be further increased by including ground truth data on areas that have been double cropped with barley (i.e. cropping barley immediately after a summer crop). The degree of discrimination between wheat and barley relates to how similar/dissimilar the temporal profile trajectories are within the cropping window (Fig. 2). The discriminatory ability of the HANTS approach seems to be weaker during wetter seasons and stronger during the drier seasons as was the case during 2003 and 2004, respectively.

**Table 2. Accuracy (%) across all classes for (i.e. wheat, barley, chickpea and non-cropping) for each method for the 2003 and 2004 seasons**

| | Per cent correctly classified (%) | | | | |
|---|---|---|---|---|---|
| | Overall | Wheat | Barley | Chickpea | Non-cropping |
| | | | *2003* | | |
| Single date | 56 | 57 | 90 | 80 | 51 |
| Multi date | 94 | 76 | 76 | 93 | 100 |
| PCA | 93 | 60 | 86 | 93 | 100 |
| HANTS | 93 | 56 | 95 | 86 | 100 |
| | | | *2004* | | |
| Single date | 61 | 74 | 85 | 100 | 56 |
| Multi date | 98 | 89 | 100 | 25 | 100 |
| PCA | 98 | 92 | 93 | 0 | 100 |
| HANTS | 95 | 85 | 71 | 0 | 100 |

This weaker discriminatory ability in wet years is likely to be related to spatial variability in rainfall and soil types, as well as the different crop-management practices, such as increased plant density rates, fertiliser application rates, or a combination of these. During 2004, which was classified as an El Niño year, there was less classification error between wheat and barley crops, resulting in more accurate area estimates at the shire scale. In addition, almost all of the area that could be planted was planted to wheat and barley, which resulted in very few ground truth fields being collated during the 2004 season. This resulted in chickpea being excluded as a feature class, which further contributed to the poor discrimination of chickpea from wheat, barley, and other crops for the 2004 season. Thus, future studies would need a large number of ground truth sampling points to enable rigorous discriminatory ability of chickpea from other winter crops.

The temporal profile trajectory represents the crop life cycle (e.g. emergence, anthesis, maturity, etc.) at a specific location and incorporates canopy reflectance responses to immediate environmental conditions (i.e. temperature, soil, moisture, light, etc.). Thus, applying these multi-temporal approaches to other geographical regions with soils and climate regimes not captured within the study area need further investigation.

### *Implications for industry*

Accurate and objective crop-area estimates are required along with yield estimates for accurate crop-production estimates. Managing storage, transport, and marketing of bulk grain commodities requires estimates of likely quantities throughout the production regions and with sufficient advance warning for appropriate responses. The proposed remote-sensing-based multi-temporal analysis approaches showed appreciable accuracy and are thus likely to be adaptable to assist industry decision-making processes and enhance handling and marketing efficiencies. This will assist the role of agri-business at national and international scales and should also be reflected in enhanced returns to growers.

Annual winter-crop production estimates can be created by incorporating the application of remote-sensing approaches, such as proposed in this study, with the end-of-season crop yield forecast issued by QDPI&F. Although end-of-year winter-crop production estimates are a significant improvement on the current ABS and ABARE survey estimates (and will be of value to industry), the need exists to generate crop area and

**Table 3. Total shire-scale area estimates and ABARE surveyed (actual) data across all features (i.e. wheat, barley, chickpea and other) for each method for the 2003 and 2004 seasons within the Jondaryan shire**
The accuracy is given in the PE (%) column, which is the difference between the estimated and actual values expressed as a percentage of the actual as collated by the ABARE survey (ABARE 2005)

| | 2003 Season | | | 2004 Season | | |
|---|---|---|---|---|---|---|
| | Estimate | Actual | PE (%) | Estimate | Actual | PE (%) |
| | | | *Single date* | | | |
| Wheat | 28597 | 27358 | 5 | 5922 | 5443 | 9 |
| Barley | 4566 | 10796 | −58 | 1853 | 2714 | −32 |
| Chickpea | 87110 | 7760 | 1023 | 18033 | 1650 | 993 |
| Winter crop | 120272 | 45914 | 162 | 25808 | 9807 | 163 |
| | | | *Multi date* | | | |
| Wheat | 74502 | 27358 | 172 | 12417 | 5443 | 128 |
| Barley | 2865 | 10796 | −73 | 7259 | 2714 | 167 |
| Chickpea | 14327 | 7760 | 85 | 0 | 1650 | −100 |
| Winter crop | 91694 | 45914 | 100 | 19676 | 9807 | 101 |
| | | | *PCA* | | | |
| Wheat | 72591 | 27358 | 165 | 8978 | 5443 | 65 |
| Barley | 2865 | 10796 | −73 | 5521 | 2714 | 103 |
| Chickpea | 6877 | 7760 | −11 | 0 | 1650 | −100 |
| Winter crop | 82334 | 45914 | 79 | 14499 | 9807 | 48 |
| | | | *HANTS* | | | |
| Wheat | 37824 | 27358 | 38 | 4909 | 5443 | −10 |
| Barley | 2674 | 10796 | −75 | 1509 | 2714 | −44 |
| Chickpea | 13850 | 7760 | 78 | 0 | 1650 | −100 |
| Winter crop | 54348 | 45914 | 18 | 6419 | 9807 | −35 |

**Table 4. Aggregated temporal (2003, 2004 and All columns) scale accuracies (MAPE, %) for each of the remote sensing analysis approaches for the study area**

| | 2003 | 2004 | All |
|---|---|---|---|
| | *Single date* | | |
| Wheat | 4 | 37 | 20 |
| Barley | 63 | 21 | 42 |
| Chickpea | 2645 | 1971 | 2308 |
| Winter crop | 182 | 268 | 225 |
| | *Multi date* | | |
| Wheat | 175 | 201 | 188 |
| Barley | 76 | 240 | 158 |
| Chickpea | 509 | 100 | 304 |
| Winter crop | 128 | 172 | 150 |
| | *PCA* | | |
| Wheat | 165 | 116 | 140 |
| Barley | 68 | 145 | 106 |
| Chickpea | 171 | 100 | 135 |
| Winter crop | 99 | 95 | 97 |
| | *HANTS* | | |
| Wheat | 43 | 15 | 29 |
| Barley | 81 | 33 | 57 |
| Chickpea | 366 | 100 | 233 |
| Winter crop | 33 | 21 | 27 |

production estimates that are available with the monthly crop yield forecast before harvest. This will avoid situations where an average crop yield is forecast (t/ha) but little to no crop could be planted because of insufficient timely rainfall events. Further research and development is necessary to address this issue of improving the lead time and frequency of accurate remote-sensing-based crop area estimates.

## Acknowledgments

We thank W. Verhoef and A. van der Kamp from the National Aerospace Laboratory (NLR) in the Netherlands for supplying the HANTS software and providing guidance and advice on its use. We also thank Land and Water Australia, through their Managing Climate Variability Program, for partly funding this project.

## References

ABARE (2005) Australian Bureau of Agricultural Resource and Economics farm survey for the 2003 and 2004. Canberra, Australia.

Campbell JB (2002) 'Introduction to remote sensing.' (Guilford Press: New York)

Department of Natural Resources and Water (2006) Queensland Land Use Mapping Program, viewed May 2005, www.nrm.qld.gov.au/science/lump.

Davis JC (2002) 'Statistics and data analysis in geology.' (John Wiley & Sons Inc.: New York)

Hammer GL, Hansen JW, Phillips JG, Mjelde JW, Hill H, Love A, Potgieter AB (2001) Advances in application of climate prediction in agriculture. *Agricultural Systems* **70**, 515–553. doi: 10.1016/S0308-521X(01)00058-0

Huete A, Didan K, Miura T, Rodriguez EP, Gao X, Ferreira LG (2002) Overview of the radiometric and biophysical performance of the MODIS vegetation indices. *Remote Sensing of Environment* **83**, 195–213. doi: 10.1016/S0034-4257(02)00096-2

Huete A, Justice C, Liu H (1994) Development of vegetation and soil indices for MODIS-EOS. *Remote Sensing of Environment* **49**, 224–234.

Huete AR, Liu HQ, Batchily K, van Leeuwen W (1997) A comparison of vegetation indices over a global set of TM images for EOS-MODIS. *Remote Sensing of Environment* **59**, 440–451.

Jakubauskas ME, Legates DR, Kastens JH (2001) Harmonic analysis of time series AVHRR NDVI data. *Photogrametric Engineering & Remote Sensing* **67**, 461–470.

Jakubauskas ME, Legates DR, Kastens JH (2002) Crop identification using harmonic analysis of time-series AVHRR NDVI data. *Computers and Electronics in Agriculture* **37**, 127–139. doi: 10.1016/S0168-1699(02)00116-3

Justice CO, Townsend JRG, Vermote EF, Masuoka E, Wolfe RE, Saleous N, Roy DP, Morisette JT (2002) An overview of MODIS Land data processing and product status. *Remote Sensing of Environment* **83**, 3–15. doi: 10.1016/S0034-4257(02)00084-6

Knopke P, O'Donnell V, Shepherd A (2000) 'Productivity growth in the Australian grains industry.' ABARE0 642 76413 1. (ABARE: Canberra)

Meinke H, Hammer GL, van Keulen H, Rabbinge R (1998) Improving wheat simulation capabilities in Australia from a cropping systems perspective. III. The integrated wheat model (I_WHEAT). *European Journal of Agronomy* **8**, 101–116. doi: 10.1016/S1161-0301(97)00015-4

Meinke H, Hammer GL, van Keulen H, Rabbinge R, Keating BA (1997) Improving wheat simulation capabilities in Australia from a cropping systems perspective. Water and nitrogen effects on spring wheat in a semi-arid environment. *European Journal of Agronomy* **7**, 75–88. doi: 10.1016/S1161-0301(97)00032-4

Muchoney D, Borak J, Chi H, Friedl M, Gopal S, Hodges J, Morrow N, Strahler A (2000) Application of MODIS global supervised classification model to vegetation and land cover mapping of Central America. *International Journal of Remote Sensing* **21**, 1115–1138. doi: 10.1080/014311600210100

Nelson RA, Holzworth DP, Hammer GL, Hayman PT (2002) Infusing the use of seasonal climate forecasting into crop management practice in North East Australia using discussion support software. *Agricultural Systems* **74**, 393–414. doi: 10.1016/S0308-521X(02)00047-1

Nix HA (1975) The Australian climate and its effects on grain yield and quality. In 'Australian field crops'. (Eds A Lazenby, EM Matheson) pp. 183–226. (Angus and Robertson: Sydney, NSW)

Penm J (2002) 'Economic overview.' Vol. 9, No. 4. (ABARE: Canberra)

Potgieter AB, Hammer GL, Butler D (2002) Spatial and temporal patterns in Australian wheat yield and their relationship with ENSO. *Australian Journal of Agricultural Research* **53**, 77–89. doi: 10.1071/AR01002

Potgieter AB, Hammer GL, Doherty A (2006) Oz-Wheat: a regional-scale crop yield simulation model for Australian wheat. Queensland Department of Primary Industries & Fisheries, Information Series No. QI06033, Brisbane, Qld (ISSN 0727-6273).

Potgieter AB, Hammer GL, deVoil P (2005) A simple regional-scale model for forecasting sorghum yield across North-Eastern Australia. *Agricultural and Forest Meteorology* **132**, 143–153. doi: 10.1016/j.agrformet.2005.07.009

Price JC (2003) Comparing MODIS and ETM + data for regional and global land classification. *Remote Sensing of Environment* **86**, 491–499. doi: 10.1016/S0034-4257(03)00127-5

Richards JA, Jia X (1999) 'An introduction to remote sensing digital image analysis.' (Springer-Verlag: Berlin, Heidelberg)

RSI (2005) Research Systems Inc. www.rsinc.com

Stephens DJ (1998) Objective criteria for estimating the severity of drought in the wheat areas of Australia. *Agricultural Systems* **57**, 333–350. doi: 10.1016/S0308-521X(98)00022-5

Stephens DJ, Butler D, Hammer GL (2000) Using seasonal climate forecasts in forecasting the Australian wheat crop. In 'Applications of seasonal climate forecasting in agriculture an natural ecosystems: The Australian experience'. (Eds GL Hammer, N Nicholls, C Mitchell) pp. 351–366. (Kluwer Academic Publishers: Dordrecht, The Netherlands)

Stone RC, Hammer GL, Marcussen T (1996) Prediction of global rainfall probabilities using phases of the Southern Oscillation Index. *Nature* **384**, 252–255. doi: 10.1038/384252a0

Verhoef W, Menenti M, Azzali S (1996) A colour composite of NOAA-AVHRR-NDVI based on time series analysis (1981–1992). *International Journal of Remote Sensing* **17**, 231–235.

Xiao X, Boles S, Liu J, Zhuang D, Frolking S, Li C, Salas W, Moore B III (2005) Mapping paddy rice agriculture in southern China using multi-temporal MODIS images. *Remote Sensing of Environment* **95**, 480–492. doi: 10.1016/j.rse.2004.12.009

Zhan X, Sohlberg RA, Townsend JRG, DiMiceli C, Carroll ML, Eastman JC, Hansen MC, DeFries RS (2002) Detection of land cover changes using MODIS 250 m data. *Remote Sensing of Environment* **83**, 336–350. doi: 10.1016/S0034-4257(02)00081-0

Zhang X, Friedl MA, Schaaf CB, Strahler AH, Hodges JCF, Gao F, Reed C, Huete A (2003) Monitoring vegetation phenology using MODIS. *Remote Sensing of Environment* **84**, 471–475. doi: 10.1016/S0034-4257(02)00135-9

Manuscript received 25 August 2006, accepted 1 February 2007